AIRCRAFT-INDUCED HOLE PUNCH AND CANAL CLOUDS

Inadvertent Cloud Seeding

BY ANDREW J. HEYMSFIELD, PATRICK C. KENNEDY, STEVE MASSIE, CARL SCHMITT, ZHIEN WANG, SAMUEL HAIMOV, AND ART RANGNO

Passage of commercial aircraft through supercooled altocumulus can induce freezing of droplets by homogenous nucleation and induce holes and channels, increasing the previously accepted range of temperatures for aviation-induced cloud effects.

The peculiar and striking formations called "hole punch" and "canal" clouds, which are sometimes seen in midlevel altocumulus, appear as circular or elongated channels or voids from which streamers of precipitation descend (Fig. 1). Altocumulus clouds are midlevel clouds that form typically at temperatures of about –15°C and are composed of water droplets, especially near cloud top, sometimes mixed with a concentration of ice particles. The features of the altocumulus in which these holes form—visual shape, cloud-top temperatures, optical depths, and cloud particle effective radii (e.g., Figs. 2a–d)—confirm that the parent clouds of the holes and canals are liquid.

Globally, midlevel liquid-layer topped stratiform clouds cover 7.8% of Earth's surface on aver-

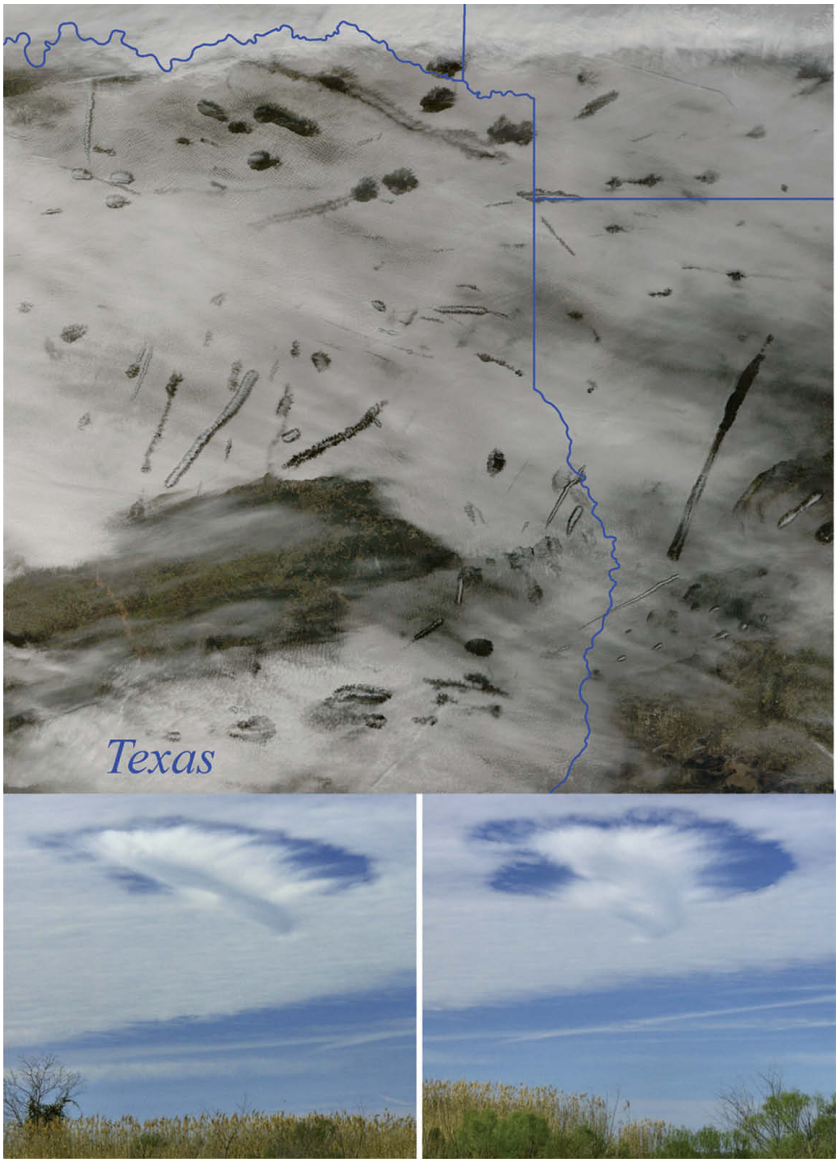

FIG. 1. (top) Image of hole punch and canal clouds captured by the Moderate Resolution Imaging Spectroradiometer (MODIS) on NASA's *Terra* satellite at 1705 UTC 29 Jan 2007 (image courtesy of NASA Earth Observatory and specifically J. Schmaltz). State boundaries are shown. (bottom) Pictures taken from near New Orleans, Louisiana, at 2110–2117 UTC 29 Jan 2007, looking northwest toward Shreveport. (Photos courtesy of Jafvis.)

age (Zhang et al. 2010). Typically, there are modest concentrations of ice in the middle atmosphere, and virga may be seen to be streaming downward from the liquid water parent cloud. However, if high ice particle concentrations are introduced by natural seeding (e. g., cirrus fallstreaks) or deliberate or inadvertent seeding, the liquid droplets in that region may disappear. According to the Bergeron–Findeisen (B-F) process, if ice is introduced into a liquid water cloud at subfreezing temperatures, the liquid droplets will be out of vapor pressure equilibrium relative to the ice and the liquid will evaporate, with vapor depositing onto the ice crystals and causing them to grow larger. This process, together with the addition of dynamical effects, can produce a visual hole or canal.

The formation mechanism(s) of hole punch and canal clouds has been the subject of conjecture based primarily on visual or satellite-borne imagery. Ice streamers nested within or falling from circular holes or elongated channels etched out of midlevel, supercooled clouds were first reported in the meteorological literature in the 1940s (Schumacher 1940). A large horizontal loop in an altocumulus, sketched in a correspondence titled "Man-made cirrus?" (*Weather* 1948), was the first of such features to be attributed to an aircraft. Early on, Ludlam (1956) likened the features to supercooled stratocumulus clouds seeded by dry-ice pellets or silver iodide smoke released from an aircraft. He suggested that the ice crystals observed within the holes could be produced by spontaneous freezing of the droplets from adiabatic cooling produced in the vortices shed by a propeller or by the rapid expansion of air at the wing tips. Spontaneous freezing or "homogeneous ice nucleation" (HN; see Bigg 1953) is a process by which droplets freeze without the need for ice nuclei, which for cloud droplets a few microns and larger occurs when the droplet temperature cools to about –37°C or below. Alternatively, Ludlam suggested that the crystals could be initiated by nuclei emitted in the engine exhaust.

In 1968, a photograph published in *Weatherwise* generated considerable interest in the "Hole-in-cloud: A meteorological whodunit?" from the U. S. meteorological community (*Weatherwise*, August 1967) and set off a round of speculation as to its cause. Most of the proposed mechanisms focused on how the unusual pattern of evaporation might have occurred, including the subsiding of air in the remnants of a hurricane's eye and local warming of the air in dissipation trails, or distrails, caused by rocket exhaust, passing meteors, or the heat produced by the passage of a jet aircraft (*Weatherwise*, February 1969, and following issues). The *Weatherwise* correspondents also suggested that jet aircraft contrails might be a source of ice particles that would grow at the expense of preexisting cloud droplets. Another report specifically implicated jet aircraft in the generation of observed hole punch clouds embedded within altocumulus (Simon 1966). The author proposed that acoustic shock waves generated by the aircraft produced the ice crystals.

Aircraft continue to be the focus of attention with respect to the generation of unusual holes in clouds. Distrails can create linear voids in clouds similar in appearance to the canals shown in Fig. 1. According to Glickman (2000), distrails are "the opposite of a condensation trail." Glickman (2000) thus describes their production: "Heat of combustion of the aircraft fuel, released into the swept path by the exhaust stacks of the aircraft, can, under certain conditions, evaporate existing clouds (if not too dense) and yield a distrail." Corfidi and Brandli (1986) observed from Geostationary Operational Environmental Satellite (GOES) imagery what they referred to as distrails in altocumulus. More recently, Duda and Minnis (2002) documented the properties of the altocumulus and ice fall streaks in two distrails observed in GOES imagery with cloud-top temperatures of –28° and –31°C. Pedgley (2008) supported earlier views that aircraft induce freezing of cloud droplets by sudden expansion and cooling to below –40°C within vortices trailing from tips of propeller blades and wings.

Currently, ice production by aircraft is conventionally considered to occur as contrails, which typically form behind jet aircraft as a result of engine combustion when the air temperature is –40°C and below, characteristic of cirrus-forming (ice cloud) conditions (Appleman 1953; Scorer and Davenport 1970). Jet aircraft fly predominantly at these temperature levels. Water vapor exhausted from an engine during com-

AFFILIATIONS: Heymsfield, Massie, and Schmitt—National Center for Atmospheric Research, Boulder, Colorado; Kennedy—Colorado State University, Fort Collins, Colorado; Wang and Haimov—University of Wyoming, Laramie, Wyoming; Rangno*—Catalina, Arizona
*Retired
CORRESPONDING AUTHOR: Andrew Heymsfield, National Center for Atmospheric Research, P.O. Box 3000, Boulder, CO 80307
E-mail: heyms1@ucar.edu

The abstract for this article can be found in this issue, following the table of contents.
DOI:10.1175/2009BAMS2905.1

In final form 4 September 2009

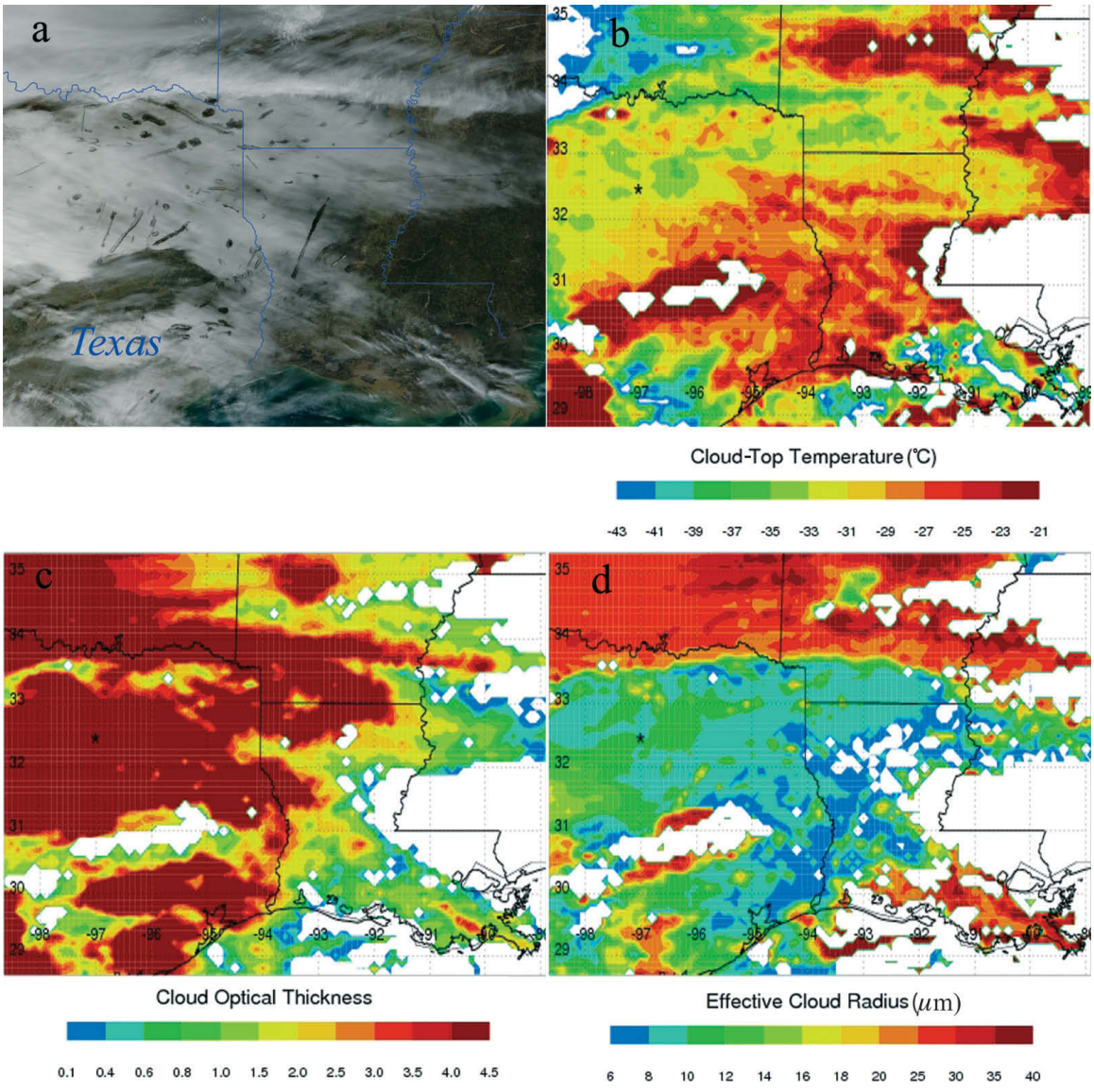

Fig. 2. Hole punch and canal clouds captured by the MODIS on NASA's *Terra* satellite on 29 Jan 2007: (a) high-resolution imagery, (b) cloud-top temperature, (c) cloud optical depth, and (d) cloud effective radius. State boundaries are shown.

bustion is rapidly condensed to droplets that almost immediately freeze to ice crystals (Appleman 1953; Brasseur and Gupta 2010). Contrail crystals falling into a supercooled cloud could dissipate droplets but not ice crystals. Although extensive contrail cirrus can form when the ambient relative humidity is in excess of saturation with respect to ice, contrail crystals usually sublimate in dry layers in the upper troposphere and thus do not generally fall into lower altocumulus clouds. Hole punch clouds are therefore not likely the result of contrails.

New calculations, supported by an observed instance, suggest that jet aircraft operating at temperatures warmer than known contrail-forming temperatures can potentially generate ice crystals. Adiabatic expansion that occurs over the upper surfaces of the wings of jet aircraft from lift can produce local cooling by some 20°C, which, under conditions of high humidity and air temperatures of –20°C and below, can produce condensation, droplet production, and then HN (Gierens et al. 2009). Jet aircraft do not typically fly in the –20° to –40°C temperature range, so the importance of this process may be restricted to climb and descent or regional jet aircraft operations.

Propeller-driven aircraft, which routinely operate at temperature levels from about –10° to below –30°C, have been shown to generate ice crystals. In the early 1980s, Rangno and Hobbs directed attention to

Fig. 3. Two B-17 Flying Fortresses' vapor trails light up the night sky over Eastern Europe, in a public domain image (www.af.mil). No details of the aircraft flight temperatures or dates of the photograph are given.

a phenomenon called aircraft-produced ice particles (APIPs). During research flights that measured cloud properties, the production of ice crystals from the passage of propeller aircraft at temperatures as warm as −8°C was documented (Rangno and Hobbs 1983, 1984). Ice particle concentrations were more than 10^4 times greater than the expected concentrations of ice nuclei at this temperature. The APIPs were contained in a relatively narrow cylindrical region of cloud; the diameter of the cylinder increased with time. The production of APIPs by a turboprop passenger aircraft flying through a stratus layer at a temperature of about −10°C was also observed (Rangno and Hobbs 1984).

Subsequently, a series of research aircraft experiments involving nine different aircraft led to an understanding of how APIPs were produced (Woodley et al. 1991, 2003). The air moving over the forward convex surfaces of a propeller generates thrust. There is a pressure difference between the forward and rear surfaces of the propeller blades, with the greatest difference at the blade tips and along the trailing surfaces. This pressure drop is responsible for propulsion, and it also causes a rapid adiabatic expansion and decrease in temperature. Droplets cool in the expanded air at the propeller tips (Fig. 3); with sufficient expansion and cooling, their temperature can drop to the point at which they freeze by the HN process. The amount of cooling and whether the temperature drops to the point of HN depends on the specifics of the aircraft's engines, the shape and number of propeller blades, and the power setting. The motivation for these carefully designed studies of APIP production was to ascertain the conditions when research and operational weather modification aircraft were influencing the clouds under study. For example, Rangno and Hobbs (1983) and Hobbs and Rangno (1984) suggested that the unexpectedly high concentrations of ice particles that were observed to develop in a maritime cloud topped at a temperature of −4°C (Mossop et al. 1968) were the result of APIPs produced by repeated penetrations by two propeller aircraft. This suggestion was vigorously defended (Mossop 1984).

The following section presents detailed observations of the development of ice produced by two turboprop aircraft and the subsequent fallout as snow to the ground as measured from an in situ aircraft penetration and coincident ground-based radar measurements. Broader impacts of ice particle production by commercial propeller and jet aircraft that operate throughout the temperature range where supercooled water may exist are explored for the first time in the discussion section.

OBSERVATIONS FROM AN EXAMPLE CASE.

On 11 December 2007, north of Fort Collins, Colorado, aircraft- and ground-based radars observed what will be shown to be a hole punch or canal cloud and the resulting precipitating ice curtain induced by the passage of two commercial passenger aircraft through a supercooled layer. The intercept occurred at coordinates 40.76°N, 104.91°W.

The data reported here were collected during the Ice in Clouds Experiment, Layer Clouds (ICE-L; www.eol.ucar.edu/projects/ice-l/). The primary goal of ICE-L was to show that, under given conditions, direct measurements of ice nuclei—the aerosols that heterogeneously initiate ice particles—can be used to predict the number of ice particles nucleating at temperatures warmer than −37°C. In situ and remote sensing data were collected from the National Science Foundation (NSF) C-130 aircraft operated by the National Center for Atmospheric Research (NCAR). The Colorado State University (CSU) Pawnee S-band radar and the National Weather Service Next Generation Weather Radar (NEXRAD) and Weather Surveillance Radar-1988 Doppler (WSR-88D), located

near Cheyenne, Wyoming, and Denver, Colorado, collected ground-based radar data. They operated at wavelengths of 10–11 cm.

The C-130 was equipped with a full complement of spectrometers to measure aerosol, cloud droplet, and ice particle size distributions (PSDs). Four probes were used to measure the PSD in sizes from 1 to 50 μm.[1] The PSDs and the cross-sectional areas for particle diameters 50–6000 μm were measured by probes that gave two-dimensional (2D) images of the particles. Redundancy and different probe designs reduced known problems and uncertainties in the measurements of small particles. The volume extinction coefficient, which is related to the visibility, was calculated from the PSDs and 2D probe imagery. Concentrations of ice nuclei (DeMott et al. 2003) and condensation nuclei were also measured. The amount of condensed (liquid + ice) water, the ice water content (IWC), was measured by a counterflow virtual impactor (CVI; Twohy et al. 1997). A 3.2-mm upward and downward Doppler cloud radar [the Wyoming Cloud Radar (WCR)] and an upward-viewing two-wavelength polarization lidar [the Wyoming Cloud Lidar (WCL)] operated by the University of Wyoming (Wang et al. 2009) provided remote sensing data. The WCR operates at a wavelength of 95 GHz, similar to the 94-GHz radar on the CloudSat satellite, and the WCL is similar to the lidar on board the Cloud-Aerosol Lidar and Infrared Pathfinder Satellite Observation (CALIPSO) satellite. Research-grade instruments for measuring the temperature, pressure, relative humidity, and air vertical motions were also on board.

Ground-based radar. An overview of the radar echo evolution at two constant altitude levels for the 1-h period ending with the arrival of the C-130 is shown in Fig. 4. The main feature of interest during this period was the development of a narrow linear echo that was first recognized in the southwest azimuth quadrant of the CSU Pawnee radar. This line echo was beginning to become defined at 5 km MSL at 1831 UTC (Fig. 4a). With time, the line echo became better defined and more reflective as larger particles developed and fell from the upper levels (Figs. 4c,e) to lower levels (3.5 km; Figs. 4b,d,f).

Flight paths recorded from aircraft operating in the general vicinity of the developing line echo were examined. It was found that a number of aircraft departing the Denver terminal area were following a standardized departure procedure that routed them over the YAMMI intersection (plotted as point Y in Fig. 4a). Two of these departures were turboprop commuter airline aircraft: a DASH-8B aircraft (Mesa Airlines, flight 7072) and a Beechcraft 1900 aircraft (Big Sky Airlines, flight 2591). The DASH-8B, with two 2150-hp turboprop engines, climbed through the 5–6-km altitude band approximately 10 min before the line echo first began to appear at the 5-km level (Figs. 4a,c). The Beechcraft 1900, with two PT6A-27 1200-hp turboprop engines, followed about 10 min later. Based on the equation developed in Woodley et al. (2003) to calculate the onset of APIP production as a function of the engine power and number of propeller blades, we estimate that these aircraft could have readily generated APIPs during their climb out through cloud, at the 5-km (–20°C) level or above.

Remote-sensing observations from C-130. From 1916 to 1930 UTC, the C-130 headed north-northeast at a constant altitude of 3.7 km MSL. The average air temperature encountered for the period was –16° ± 0.8°C. From 1920 to 1923 UTC, the WCR detected light snow precipitating from the layer 1.5 km above the C-130's height to the ground (Figs. 5a,b). The lidar backscattered power from 1920 to 1923 UTC maximized in a layer 200-m thick, beginning approximately at a height of 1.25 km above the C-130 (Fig. 5c). The lidar beam was fully attenuated in only a 200-m path through this layer. Because there was relatively little ice (Fig. 5a), the abrupt occultation indicated that this was a liquid water layer.

From 1923:31 to 1923:40 UTC, the WCR cloud radar detected the line echo as a discrete, continuous entity extending from about 0.5 km above the C-130's altitude to the ground (Figs. 5a,b). The Pawnee radar confirmed that the C-130 penetrated the line echo at this position. The C-130 crossed the line echo at about 1923:31 to 1923:42 UTC, where the high reflectivity was noted in the downward-looking radar imagery (Fig. 5b). Particle images showed that this reflectivity coincided with precipitation-size ice particles (Fig. 5d).

Just south of the line echo, from 1922:57 to 1923:39 UTC, the forward-viewing camera on the C-130 continuously detected a hole in the overlying altocumulus cloud (Fig. 6a). There was a clear view of this feature beginning at least 7 km before it was underflown. No such feature was observed at other times during the period. The 1-Hz images from the forward-viewing camera were used to map out the

[1] The probes included a forward-scattering spectrometer probe (FSSP; 0.8–50 μm), an open-path cloud droplet probe (CDP; 3–43 μm), an open-path small ice detector (SID) probe (1–46 μm), and a cloud particle imager (CPI) probe.

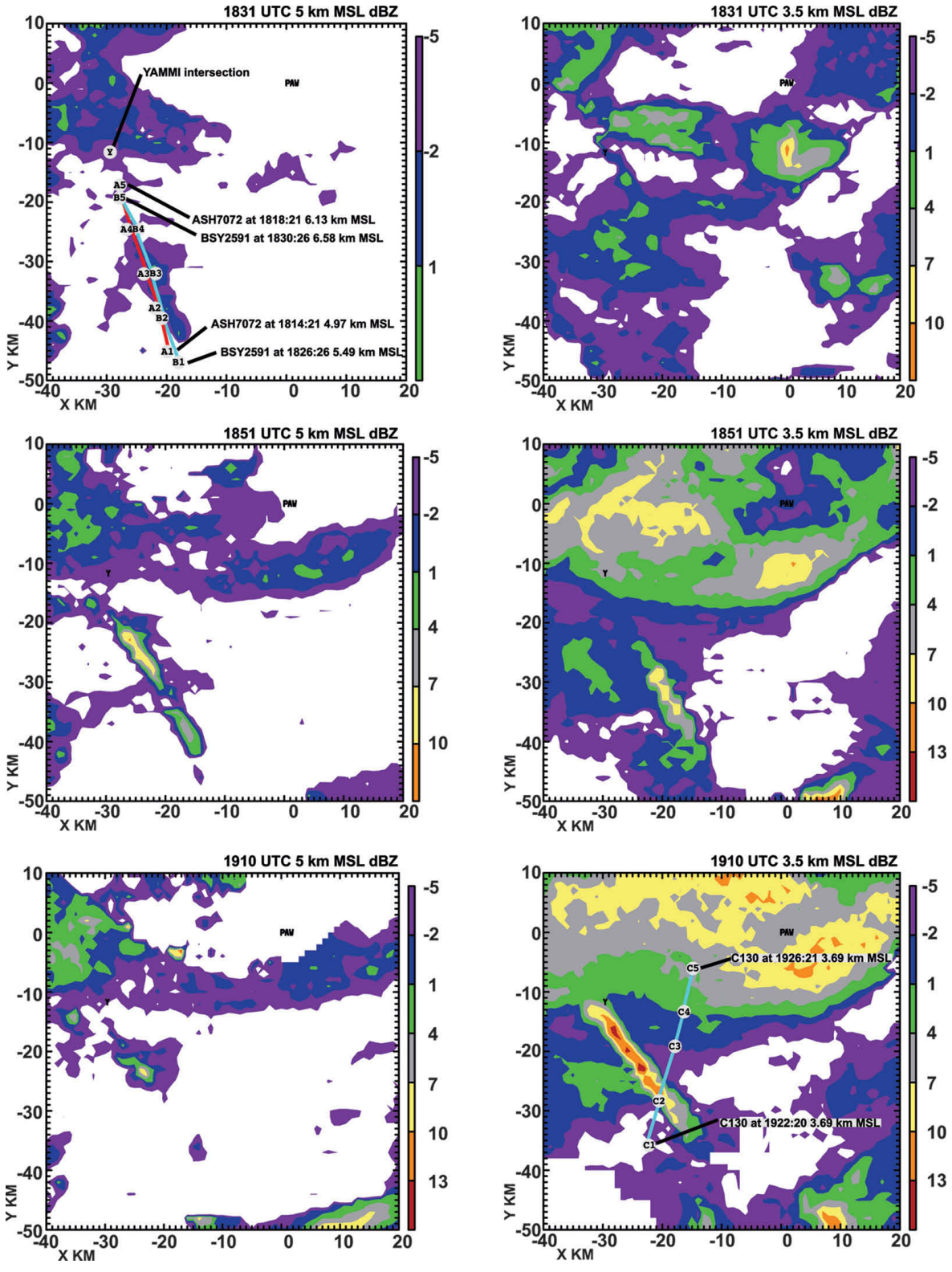

Fig. 4. Ground-based radar observations for the example case on 11 Dec 2007. Radar reflectivities measured at constant altitudes of (left) 5 and (right) 3.5 km MSL as a function of time: (top) 1831, (middle) 1851, and (bottom) 1910 UTC. The reflectivity data were interpolated to a series of constant height planes with a horizontal spacing of 1 km. The CSU Pawnee radar (point PAW) and YAMMI intersection (point Y) are plotted. Tracks of the two aircraft that likely produced the line echoes are shown in the top left panel; the C-130 track is shown in the bottom right panel.

position and size of the hole photogrammetrically. The hole was 1 km in length from north to south and 1.8 km perpendicular to the C-130 track, or along the track of the commercial aircraft. The hole was wider than the aircraft path, indicating that microphysics or some dynamical feedback mechanism was widening it. Its bottom was located about 1 km above the C-130. Based on the ground speed, the aircraft reached a point below the hole at the position shown by a red square in Fig. 6a. The downward-viewing camera was briefly obscured by a burst of precipitation coinciding with the radar observation of this enhanced reflectivity region (Fig. 6b). The blue-colored minima above the lidar line echo indicate areas devoid of ice (Fig. 6c). We suggest that the ice that formed the line echo swept out the ice in its path as the snow that formed in the hole descended toward the aircraft level. The ice in the line echo partially attenuated the lidar beam, as noted from the weakness in the liquid cloud layer above. The lidar imagery at high resolution identifies a region devoid of liquid water as ascertained from the WCL signal in the photogrammetrically determined hole punch location (red square in Figs. 6b–d). Lidar depolarization (Fig. 6d) can be used to ascertain whether the white area about 1.75 km above the C-130 height in the layer associated with the hole punch is indeed dominated by liquid water. Because there is strong backscatter, a low depolarization ratio near the base of the layer, and a gradually increasing depolarization ratio as the laser penetrated deep into water layer resulting from multiple scattering or the lidar beam, it can be concluded that this is a layer of liquid water (Wang et al. 2009).

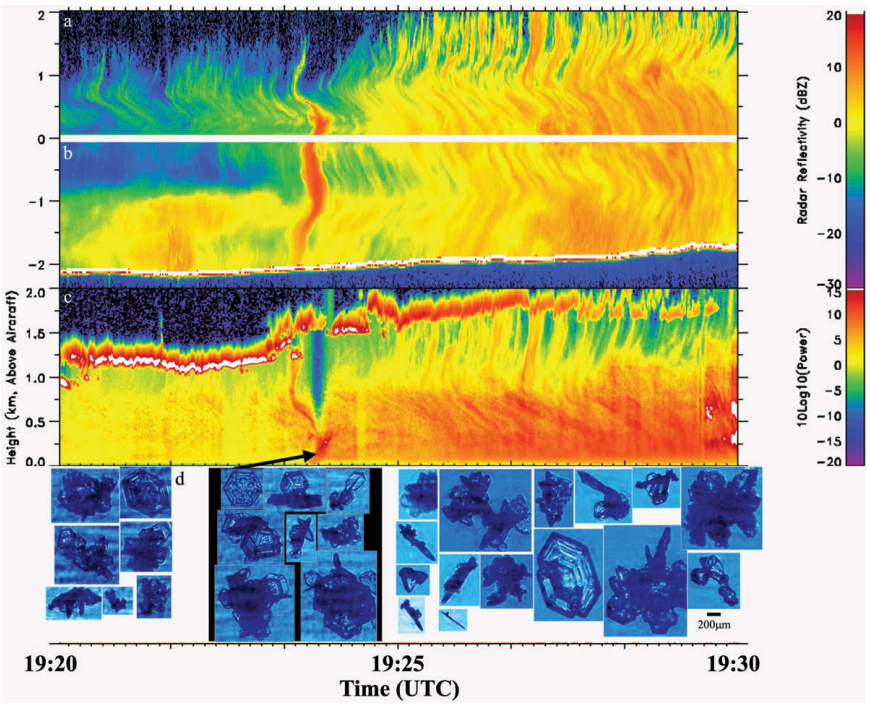

Fig. 5. Radar reflectivity from WCR 95-GHz radar (a) zenith and (b) nadir viewing. Height is altitude above or below the C-130 altitude. (c) WCL lidar, zenith viewing. (d) Images of ice crystals sampled by the CPI probe. The scale is shown. Particles overlaying the black background were observed within the line echo. Note the hole in precipitation above where the line echo crystals were intercepted. Light snow precipitation was falling from the layer 1.5 km above the C-130's height.

The radar Doppler velocities indicated that, in the mean, the ice particles were falling at about 0.75 m s^{-1} just above the aircraft to 1 m s^{-1} below it (not shown). To fall the 1.5 km from the liquid water layer to the C-130 height would require a minimum of 2000 s, because fall speeds are much lower during early particle growth. For this reason and given the location of the line echo, we surmise that the C-130 penetrated the line echo due to APIPs produced by one or both of the turboprop aircraft.

Microphysical observations. Ice particles sampled in the streamers before and after the line echo was penetrated were spatial-type plates, plates, and aggregates of spatial plates (Figs. 5d, 7). Spatial plates form at temperatures near –25°C. The temperature in the liquid water layer was within a few degrees of this, as suggested from the soundings (Fig. 8a). Many of the ice particles observed in the streamers collected droplets during their growth. The light to moderate "riming" of the ice proves the existence of a liquid water layer, almost certainly at the heights where the line echo originated but outside of it. Although the morphology of the ice within the line echo was the same as outside of it, in sharp contrast the particles in the line echo were for the most part pristine and not rimed (Figs. 5d, 7), with large plate-like features extending from them. Preexisting droplets in what became the line echo were evidently evaporated as a result of the B-F process.

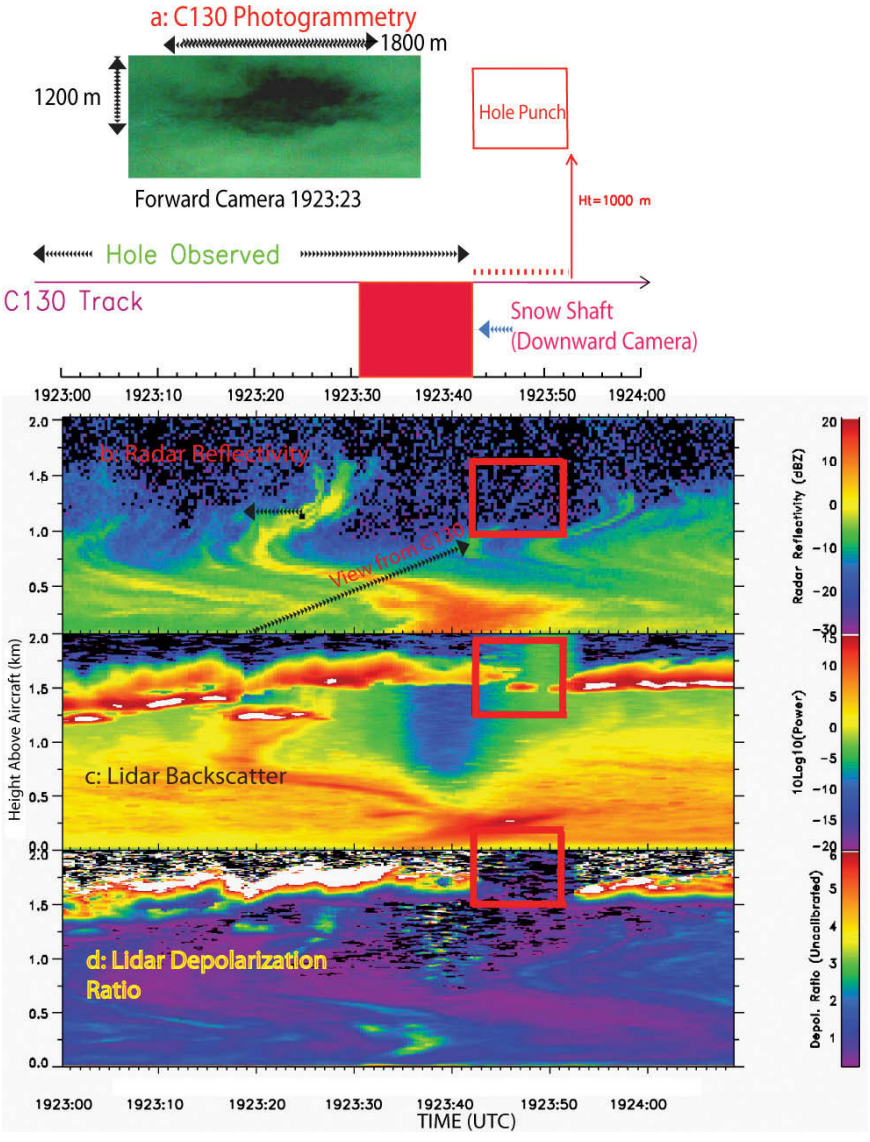

Fig. 6. Depiction of one minute of C-130 data during the line crossing. (a) Enhanced forward-looking camera digital photograph; the hole punch location is derived photogrammetrically (red box); and the snow shaft is located where the ground is not visible from the downward-looking camera. (b) Upward-viewing C-130 radar. Lidar (c) relative returned power and (d) uncalibrated (relative) depolarization ratio. Red squares indicate the approximate location of the hole punch cloud.

The thermodynamic stability of a layer can be characterized from the equivalent potential temperature (θ_e; Fig. 8b). The layer from 2.8 km to about 5.2 km, which contains the line echo, is stable, because θ_e increases with height. Between heights of 5.2 and 6.0 km, θ_e is nearly constant. If taken from a relative humidity of 100% with respect to water to 100% with respect to ice, a liquid water layer at –25°C would release 0.15 g m^{-3} IWC, with slightly more added by any liquid water that may have been present. Latent heating resulting from the ice growth would increase the temperature in that region by at least 0.6°C, enough to produce local overturning in the generation layer. The IWC sampled at the C-130 altitude was in broad agreement with these approximations (Fig. 8c). The line echo had relatively high IWCs compared to those found in the streamers. Thus, ice production was more efficient because of the aircraft-induced seeding of the liquid layer.

The volume extinction coefficient σ in 2D probe sizes is also relatively high in the line echo compared to those found in the streamers (Figs. 8c,d). Taking 0.004 m^{-1} as the value of σ in the line echo (Fig. 8d), the 0.5-km-deep layer of line echo above the C-130 altitude would give an optical depth τ of 2.0. Contributions from the small, 2–50-μm particles would add less than 1 to the value of τ. This degree of occultation can account for some but not all of the signal power loss measured by the lidar in Figs. 5c and 6c. Therefore, the "blue shadow" represents a mostly ice-free region. The continuously observed hole feature seen in the forward-looking video camera imagery supports this result.

Particle size distributions were measured at a rate of 1 Hz throughout the flight. For brevity, we choose to show a comparison of the averaged size distributions and total concentrations measured in the streamers located to the south of the line echo with those within it. The cloud north of the line echo is higher and therefore less representative of the conditions in the cloud where the hole punch was formed. The most notable findings are 1) the almost two orders of magnitude larger concentrations of small,

<75-μm particles sampled with a number of probes in the line echo when compared with those particles sampled outside of the echo; 2) the factor of 15 higher concentrations of >50-μm (2D) particles in the line echo; and 3) the bimodality of the size distribution in the 2D probe size particles in the line echo, with the second mode beginning at about 500 μm. In many years of collecting PSDs, we have rarely—if ever—seen this feature. It suggests that there may have been a naturally produced ice precipitation streamer (see Fig. 6b) superimposed on a population of aircraft-produced ice particles.

The concentration of natural ice nuclei on this day was about 1 L^{-1} at –20°C at water saturation, as measured by a continuous flow diffusion chamber (DeMott et al. 2003). Somewhat higher concentrations would be expected at –25°C. The total concentrations measured in the ice precipitation streamers were on the order of 1 L^{-1}, which is consistent with the background concentration of ice nuclei. Residuals of the sublimated ice particles in the line echo as measured by mass spectrometers on the C-130 indicate that combustion product aerosols did not play an appreciable role in ice nucleation. There was no enhancement in the concentrations of condensation nuclei across the line echo. In this event, we conclude that APIPs generated at the propeller tips were more important for ice production than ice nuclei enhancement related to engine exhaust products. This conclusion may not apply to lower formation temperatures, where exhaust products may be important.

DISCUSSION. We suggest that hole punch and canal clouds are produced in an environment of supercooled midlevel clouds as a consequence of the homogeneous freezing of cloud droplets to ice crystals in air undergoing adiabatic expansion produced by an aircraft. The concentrations of the ice crystals produced are much higher than the ambient concentrations and consume cloud droplets via the Bergeron–Findeisen process.

The long canals (e.g., Fig. 1) argue for continuous production of ice crystals at cruise altitudes via adiabatic expansion; our observations and those of Woodley et al. (2003) do not implicate combustion products. These canals are similar in appearance to the voids referred to as distrails and may be confused with them. In the case of turboprop aircraft, cooling occurs in air expanded by thrust generated at the propeller tips. When a turboprop aircraft is flown with the landing gear and flaps retracted, as was the case for earlier studies of APIPs, ice is produced beginning at temperatures as warm as –8°C. At cruise conditions, the onset of APIPs is merely de-

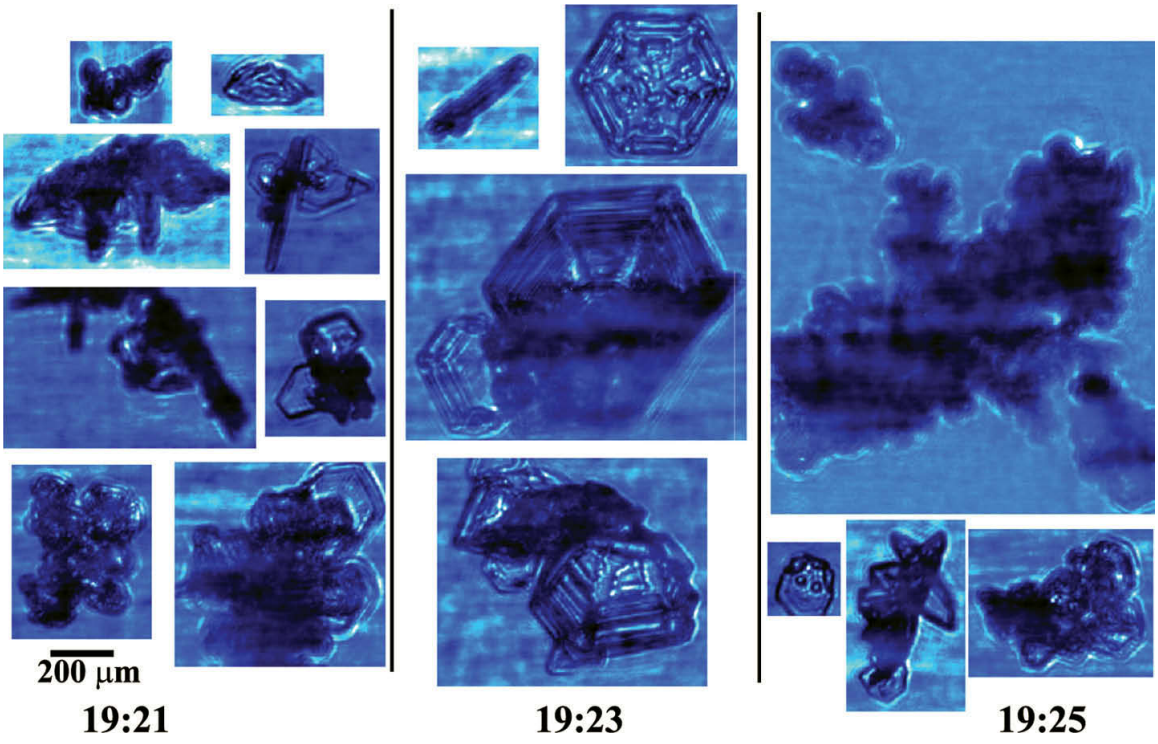

Fig. 7. As in Fig. 5d, but with higher resolution, showing ice crystals in and around the snow precipitating from the hole punch cloud.

layed to temperatures a few degrees lower than when operating at nearly full power or to temperatures of about –15°C, depending on the aircraft involved (see Woodley et al. 1991, 2003). More studies of specific aircraft are clearly warranted to characterize these conditions. Because this phenomenon is related to propeller and not jet aircraft, we refer to them as propeller-produced ice particles (PPIPs).

Adiabatic expansion over the upper surfaces of an aircraft wing can also produce appreciable adiabatic

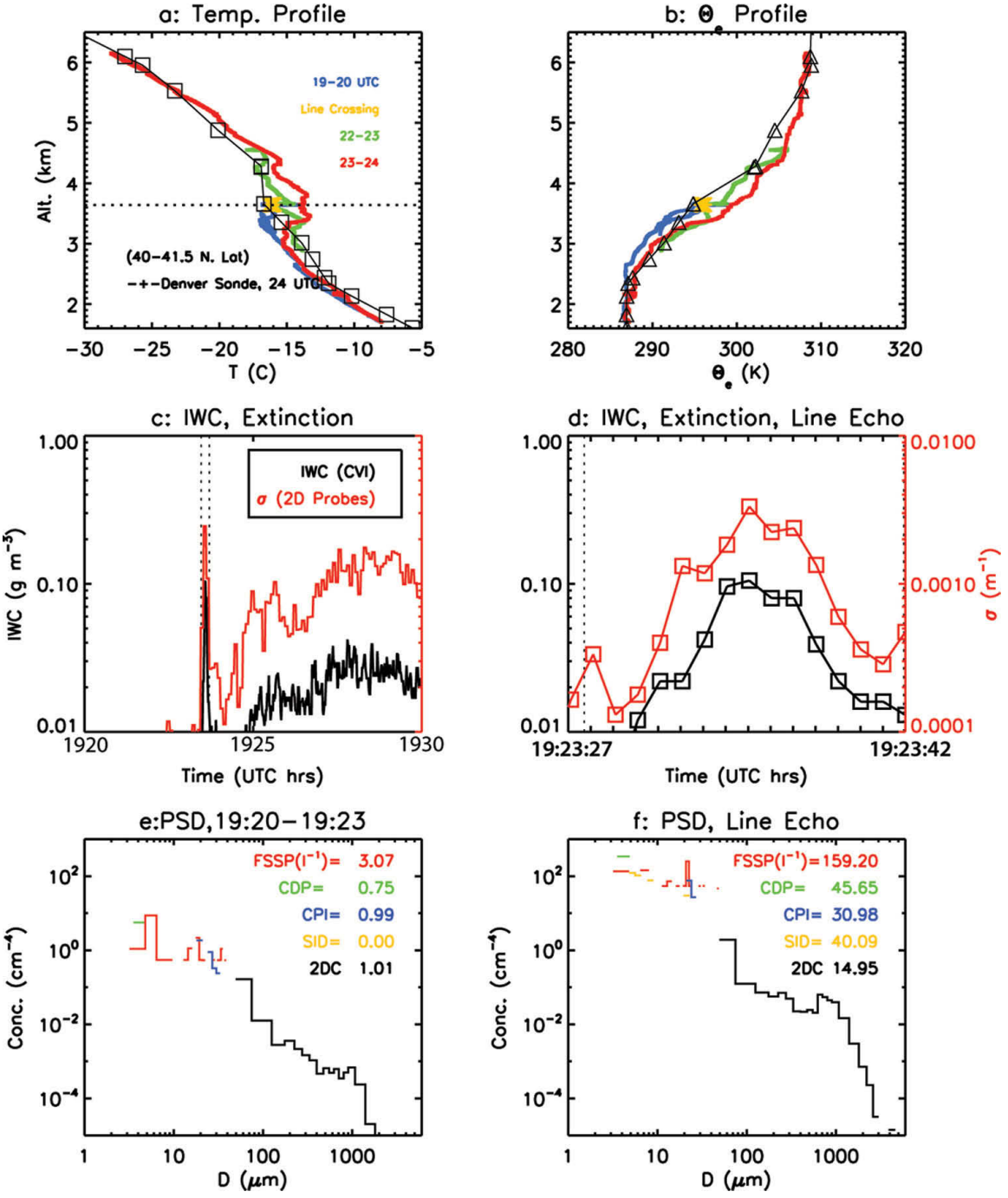

Fig. 8. C-130 observations on 11 Dec 2007. (a) Temperature profiles geographically close to the line echo, with the crossing of the line highlighted. (b) Equivalent potential temperature. IWC measured with a CVI probe and extinction derived from the 2D probe data for (c) the period that includes the line echo crossing and (d) the line echo crossing. Boxes are separated in time by 1 s. Average PSDs measured in precipitation streamers (e) south of the line echo and (f) for the line echo. Total concentrations measured by each probe are listed.

cooling and condensation under suitable conditions. Airline passengers observe this condensation in the form of visible vortices that trail from the wing tips and wing flaps of aircraft during landing or takeoff in humid conditions. Lifting-induced condensation can occur anywhere in the atmosphere under suitably humid conditions. The amount of adiabatic cooling is proportional to the wing loading—the loaded weight of an aircraft divided by the area of the wing. The drop in pressure over the top of a wing, thus the amount of adiabatic cooling, is proportional to the wing loading. Gierens et al. (2009) calculate that the air lifted over the wing of a jet aircraft cools by as much as 12°–20°C at jet aircraft altitudes, which can be sufficient to produce ice crystals by the HN process. This effect can potentially occur immediately above, below, or within a supercooled cloud. If the relative humidity in the environment is above 100% with respect to ice, then the ice crystals produced via this process will grow. If produced within a supercooled cloud, then the B-F process will deplete the droplets.

Two examples of visible condensation and subsequent ice production produced by adiabatic cooling from the lifting surfaces of jet aircraft are shown in Figs. 9 and 10. Figure 9a shows the early stage of what appears to be a contrail in or immediately below an altocumulus deck, as determined from the cloud structure and absence of ice optical phenomena. This contrail was evidently produced by a jet aircraft flying over Seattle, Washington, from west to east. Ice is produced (Figs. 9b,c), a canal cloud forms (Fig. 9d), and the altocumulus dissipates (Figs. 9e,f). The ice particles are more resistant to the evaporation process than the droplets that constituted the preexisting altocumulus, and they remain visible after the cloud dissipates. The ice trail in Fig. 10 was produced immediately below an altocumulus layer with bottom and top temperatures measured by a research aircraft of –20° and –22°C, respectively. The pilot of the research aircraft observed that a DC-9 jet aircraft produced this trail during its descent for landing, and the onboard scientist later observed ice optical phenomena in the ice trail. As with the first observation of canal clouds known to be produced by jet aircraft (Simon 1966), in both of these events adiabatically induced cooling due to the passage of jet aircraft resulted in the appearance of a visible ice trail at temperatures much above traditional temperatures defined by Appleman criteria (Appleman 1953). We refer to the production of ice over the wings as wing-produced ice particles (WPIPs).

Jets are more likely than turboprop aircraft to produce aerodynamic contrails because of their higher wing loading and flight speeds. Calculations for the NCAR C-130 turboprop aircraft wing indicates that cooling over the wing surfaces is only about 2°C for its normal airspeeds of about Mach 0.4, whereas if the C-130 flew at Mach 0.8 the cooling would be more than 20°C (K. Gierens 2009, personal communication). Therefore, the amount of cooling is higher for jet aircraft than for turboprops, because jet aircraft fly faster and they have higher wing loadings. Ice production by jet aircraft via aerodynamic contrails is more restrictive than APIP production by propeller aircraft, because the amount of cooling by adiabatic expansion is less and jet aircraft generally fly at temperatures of –37°C and below, where there are no supercooled cloud droplets; nonetheless, regional jet aircraft, which tend to cruise at somewhat lower altitudes, may be more amenable to WPIP production.

For the cloud depicted in Fig. 1, temperatures were in the range of about –25° to –30°C in most locations where the hole punch and canal clouds were observed (see Fig. 2b). We have analyzed soundings from several sites in the area covered by the figure. Where possible, we objectively corrected the soundings for dry biases often noted at low temperatures. A thin layer with humidities close to water saturation was noted near –31°C. These conditions are consistent with the limit of the amount of cooling that jet aircraft can produce aerodynamically (Gierens 2009), but at temperatures above the normal cruise conditions for jet aircraft. Thus, both turboprop and jet aircraft were fully capable of producing the temperature drops necessary to reach the –37°C temperature required for homogeneous ice nucleation in this unusual situation, where supercooled water was present at very low temperatures over an extensive area. Cirrus clouds were not overlying the holes and canals; therefore, in this instance, ice streamers were not naturally seeding the altocumulus clouds from above.

Although turboprop and jet aircraft can each produce hole punch and canal clouds through the B-F process, aircraft wake vortex dynamics must also be considered in their production. At altocumulus heights, typical turboprop aircraft force down air in their wake by approximately 150 m and jet aircraft force down air by 400 m or more over a lateral distance corresponding to the aircraft's wingspan or wider (D. Lewellen 2009, personal communication). Wing vortex dynamics would act to evaporate cloud drops in an altocumulus. Taking reasonable altocumulus liquid water contents (LWCs) of 0.01, 0.05, and 0.1 g m^{-3} at a temperature of –25°C, descents of air in wake vortices by only 20, 100, and 200 m, respectively, will fully evaporate the droplets; at –15°C, only 13, 60, and

Fig. 9. Sequence showing the production of what appears to be a contrail in or below an altocumulus deck, the formation of ice and a canal cloud, and the dissipation of the altocumulus layer with the residual ice layer.

110 m are required. In only a few minutes following the passage of an aircraft, therefore, a wake vortex dynamics could produce a hole or canal, albeit narrow.

Following droplet evaporation, with continued descent of the now dry air in the vortex, small ice crystals could sublimate. Lewellen and Lewellen (2001) concluded from a modeling study that there is appreciable loss of contrail ice particles in wake vortices. To evaluate this possibility, we ran modeling calculations using the parcel descent distances mentioned earlier and the range of temperatures where PPIPs and WPIPs are produced. We conclude that wake vortex descent probably does not result in appreciable ice sublimation.

SUMMARY AND CONCLUSIONS. Ice crystals can be produced by both turboprop and jet aircraft

in and around supercooled liquid cloud layers. These crystals are produced by local adiabatic expansion at propeller tips at temperatures as warm as −8°C or over wing surfaces at temperatures <–20°C, and the resultant cooling chills droplets to a temperature of –37°C or below, causing the supercooled droplets to freeze via homogeneous nucleation. Through the Bergeron–Findeisen process, the ice crystals grow rapidly at the expense of the supercooled drops in the preexisting cloud layer. Our observations for the ICE-L case clearly demonstrate that this process can lead to linear, precipitating columns of ice composed of a high concentration of ice particles, some growing to sizes of 1 mm and larger, with a detectable radar echo.

Wake turbulence is sufficient to produce holes of the size initially seen, but is unable to induce further spread (Pedgley, 2008). As an aircraft ascends into or flies through a supercooled altocumulus, a hole or canal may be produced by aircraft wake vortex descent. However, when visual/optical indications of ice particles remain in the centers of the holes or channels, it is improbable that the clearings were caused by wake vortex–induced downward motions. In the absence of naturally occurring ice particle sources (fall streaks from overlying cirrus clouds, etc.), the ice particles introduced by aircraft are probably responsible for many of the hole and channel openings observed in widespread supercooled altocumulus cloud decks.

Three factors may serve to widen the initial hole or channel with time: 1) dispersion of the aircraft's exhaust trail, which spreads the ice trail laterally with time t (in seconds) at a distance on the order of $4t^{0.5}$, or only about 200 m in 30 min (see Schumann et al. 1995); 2) a manifestation of the B-F process, with the consequence that droplets at the edges of the ice/drop interface would continue to evaporate with time; and 3) the net result of latent heating from ice growth, increasing the temperature in the hole. This latter mechanism would produce a locally warm region in a layer of neutral buoyancy, typical of altocumulus, forcing the air in the hole to rise and the air around it to subside. Transport of ice in this circulation and the subsidence in the liquid water region would further erode the surrounding liquid cloud. Whether a hole punch or canal cloud is formed—the channel's aspect ratio—depends on the thickness of the cloud (time for the aircraft to climb through it), the thermodynamic stability and vertical and horizontal wind shear, and the air temperature. Of course, there may be situations where a hole is produced naturally: for example, by ice streamers falling from cirrus clouds above.

In effect, aircraft have the potential to inadvertently seed supercooled cloud layers. Figure 1 shows only the effect that aircraft can have on certain thin, liquid water clouds. Whether hole punch or canal clouds are detectable from the ground or from satellite observations depends on the presence of intervening cloud, background cloud on the opposite side of the feature, and/or flight through preexisting radar echo. However, the question of detectability surely leads us to conclude that numerous aircraft effects on clouds and precipitation occur unnoticed in deeper clouds when the signal is not so obvious. What are those effects? More extensive studies are needed to characterize regional implications of aircraft interactions with supercooled cloud layers. For the research community, because ice nucleation in maritime clouds is of considerable significance, follow-up observations that document unexpectedly high ice concentrations and glaciation of maritime clouds at warm temperatures (Mossop et al. 1968) are of vital importance for understanding current and future climates.

Fig. 10. The production of a contrail by a DC-9 aircraft descending through an altocumulus layer with base and top temperatures of −20° and −22°C respectively.

ACKNOWLEDGMENTS. We wish to thank Jafvis for his original photographs of hole punch clouds, Jeff Schmaltz for preparing MODIS images, and the NASA Earth Observatory (http://earthobservatory.nasa.gov) for the use the original MODIS data. Insights into aerodynamic contrail production by Klaus Gierens and APIPs with William Woodley were invaluable. Data processing and figure preparation by Jason Craig, Nathan Downs, and Lara Ziady and original data provided by Cynthia Twohy and Paul DeMott are appreciated. Paul Field is acknowledged for his contributions to the ICE-L field program. The support of the NCAR Research Aviation Facility, especially Jorgen Jensen, Jeff Stith, Dave Rogers, Henry Boynton, Ed Ringleman, and Stuart Beaton, was indispensable. Meg Miller provided editorial assistance. Thanks are also given to Steve Rutledge and the CSU–CHILL team for their Pawnee radar support. CSU ground-based radar research activities are supported by NSF Cooperative Agreement ATM 0735110. This research was supported by the National Science Foundation.

REFERENCES

Appleman, H., 1953: The formation of exhaust condensation trails by jet aircraft. *Bull. Amer. Meteor. Soc.,* **34,** 14–20.

Bigg, E. K., 1953: The supercooling of water. *Proc. Phys. Soc.,* **66B,** 688–694.

Brasseur, G., and M. Gupta, 2010: Impact of aviation on climate: Research priorities. *Bull. Amer. Meteor. Soc.,* **91,** 461–463.

Corfidi, S., and H. W. Brandli, 1986: GOES views aircraft distrails. *Natl. Wea. Dig.,* **11,** 37–39.

DeMott, P. J., K. Sassen, M. R. Poellot, D. Baumgardner, D. C. Rogers, S. D. Brooks, A. J. Prenni, and S. M. Kreidenweis, 2003: African dust aerosols as atmospheric ice nuclei. *Geophys. Res. Lett.,* **30,** 1732, doi:10.1029/2003GL017410.

Duda, D. P., and P. Minnis, 2002: Observations of aircraft dissipation trails from GOES. *Mon. Wea. Rev.,* **130,** 398–406.

Gierens, K., B. Kärcher, H. Mannstein, and B. Mayer, 2009: Aerodynamic contrails: Phenomenology and flow physics. *J. Atmos. Sci.,* **66,** 217–226.

Glickman, T., Ed., 2000: *Glossary of Meteorology.* 2nd ed. Amer. Meteor. Soc., 855 pp.

Hobbs, P. V., and A. L. Rangno, 1984: Reply. *J. Climate Appl. Meteor.,* **23,** 346.

Lewellen, D. C., and W. S. Lewellen. 2001: The effects of aircraft wake dynamics on contrail development. *J. Atmos. Sci.,* **58,** 390–406.

Ludlam, F. H., 1956: Fall-streak holes. *Weather,* **11,** 89–90.

Mossop, S. C., 1984: Comments on "Production of ice particles in clouds due to aircraft penetrations." *J. Climate Appl. Meteor.,* **23,** 345–345.

——, R. E. Ruskin, and K. J. Heffernan, 1968: Glaciation of a cumulus cloud at approximately –4°C. *J. Atmos. Sci.,* **25,** 889.

Pedgley, D. E., 2008: Some thoughts on fallstreak holes. *Weather,* **63,** 356–360.

Rangno, A. L., and P. V. Hobbs, 1983: Production of ice particles in clouds due to aircraft penetrations. *J. Climate Appl. Meteor.,* **22,** 214–232.

——, and ——, 1984: Further observations of the production of ice particles in clouds by aircraft. *J. Climate Appl. Meteor.,* **23,** 985–987.

Schumacher, V. C., 1940: Beobacktungen an einer Altokumulusdecke (Observations in an altocumulus layer). *Z. Angew. Meteor.,* **57**, 214.

Schumann, U., P. Konopka, R. Baumann, R. Busen, T. Gerz, H. Schlager, P. Schulte, and H. Volkert, 1995: Estimate of diffusion parameters of aircraft exhaust plumes near the tropopause from nitric oxide and turbulence measurements. *J. Geophys. Res.,* **100,** 14 147–14 162.

Scorer, R. S., and L. J. Davenport, 1970: Contrails and aircraft downwash. *J. Fluid. Mech.,* **43,** 451–464.

Simon, A., 1966: Dissipation d'un altocumulus sur le pasage d'un avion a reaction (Dissipation of an altocumulus by the passage of a jet aircraft). *J. Rech. Atmos.,* **2,** 36–38.

Twohy, C. H., A. J. Schanot, and W. A. Cooper, 1997: Measurement of condensed water content in liquid and ice clouds using an airborne counterflow virtual impactor. *J. Atmos. Oceanic Technol.,* **14,** 197–202.

Wang, Z., P. Wechsler, W. Kuestner, J. French, A. Rodi, B. Glover, M. Burkhart, and D. Lukens, 2009: Wyoming cloud lidar: Instrument description and applications. *Opt. Express,* **17,** 13 576–13 587.

Weather, 1948: Man-made cirrus? *Weather*, **3,** 232.

Woodley, W. L., T. J. Henderson, B. Vonnegut, G. Gordon, R. Breidenthal and S. M. Holle, 1991: Aircraft-produced ice particles (APIPs) in supercooled clouds and the probable mechanism for their production. *J. Appl. Meteor.,* **30,** 1469–1489.

——, and Coauthors, 2003: Aircraft-produced ice particles (APIPs): Additional results and further insights. *J. Appl. Meteor.,* **42,** 640–651.

Zhang, D., Z. Wang, and D. Liu, 2010: A global view of midlevel liquid layer topped stratiform cloud distributions from CALIPSO and CloudSat measurement. *J. Geophy. Res.*, **115,** D00H13, doi:10.1029/2009JD012143.